Journal of Zhejiang University SCIENCE A
ISSN 1009-3095 (Print); ISSN 1862-1775 (Online)
www.zju.edu.cn/jzus; www.springerlink.com
E-mail: jzus@zju.edu.cn

# Analysis of structural response under blast loads using the coupled SPH-FEM approach*

Jun-xiang XU†, Xi-la LIU

(*Department of Civil Engineering, Shanghai Jiao Tong University, Shanghai 200240, China*)

†E-mail: xujunx@msn.com

Received Nov. 25, 2007; revision accepted Feb. 25, 2008

**Abstract:** A numerical model using the coupled smoothed particle hydrodynamics-finite element method (SPH-FEM) approach is presented for analysis of structures under blast loads. The analyses on two numerical cases, one for free field explosive and the other for structural response under blast loads, are performed to model the whole processes from the propagation of the pressure wave to the response of structures. Based on the simulation, it is concluded that this model can be used for reasonably accurate explosive analysis of structures. The resulting information would be valuable for protecting structures under blast loads.

**Key words:** Smoothed particle hydrodynamics (SPH), Finite element method (FEM), Reinforced concrete structure, Explosion
**doi:**10.1631/jzus.A0720080 **Document code:** A **CLC number:** TU312

## INTRODUCTION

The response of structures subjected to blast loads is a complicated process. Many researches on this field have been reported (Lu and Jiang, 2001; Luccioni *et al.*, 2004; Du *et al.*, 2006). Among them, the numerical simulation has been paid extensive attention.

In the traditional finite element method (FEM), the numerical mesh moves and deforms with the physical material. Free surface and material interfaces are located at element boundaries and hence can be maintained throughout the calculation. Therefore, FEM is well suited for solid material. However, due to large deformation and chuck of soil near the charges, the computational difficulty for FEM resulted from mesh distortion will occur in explosive analysis.

Smoothed particle hydrodynamics (SPH) is a meshless, particle method of Lagrangian nature (Liu *et al.*, 2003). It has a natural advantage over meshed methods for problems in which topologically discontinuous deformations such as collapse, fracture, and fragmentation occur. SPH not only overcomes the aforementioned grid tangling problem of FEM under extreme deformations, but also can easily track the material boundary and history dependent behavior. However, accurate SPH simulations require uniformly sized particles throughout the SPH region. Hence if high accuracy is sought in numerical simulations, large run time can be a problem (Century Dynamic Inc., 1998). On the other hand, the implementation of boundary conditions in particle methods is not so clearly defined as it is with meshed methods.

A combination of FEM and SPH will be especially effective for modeling the process involving the formation of craters by the explosion, the propagation of pressure and the response of structures. The basic idea is to couple SPH with FEM elements through the definition of interaction between them. In the present study, SPH is used to model explosion charges and the near field with large deformation resulted from blast loads, while FEM elements are used to model the far medium including the building.

In Section 2, the coupled SPH-FEM approach is employed to explosive analysis of free field. Simulation results are compared with empirical equations to validate the material model and the coupled method.

* Project supported by National Basic Research Program (973) of China (No. 2002CB412709) and the National Natural Science Foundation of China (No. 50378054)

Then, based on the obtained results, the response of the structure subjected to subsurface blast is studied and finally some conclusions are drawn. The explicit hydrocodes Autodyn is used for the calculations.

## COUPLED SPH-FEM APPROACH

### SPH basis

The SPH technique was first developed in astrophysics by Lucy (1977) and Gingold and Monaghan (1977). In early 1990s, it was applied to the simulation of elasticity and fragmentation in solids. In this method, the state of a system is represented by arbitrarily distributed particles, which carry all the computational information including mass and velocity as well as elastic modulus. Using the concept of kernel and particle approximation, the discretized SPH equations of motion for numerical simulation of blast analysis are given as follows.

Conservation equation of mass:

$$\frac{\mathrm{d}\rho}{\mathrm{d}t}(\boldsymbol{x}_i)=\sum_{j=1}^{N}m_j(v(\boldsymbol{x}_j)-\boldsymbol{v}(\boldsymbol{x}_i))A_{ij}. \tag{1}$$

Conservation equation of momentum:

$$\frac{\mathrm{d}\boldsymbol{v}^{\alpha}}{\mathrm{d}t}(\boldsymbol{x}_i)=\sum_{j=1}^{N}m_j\left\{\frac{\boldsymbol{\sigma}^{\alpha,\beta}(\boldsymbol{x}_j)}{\rho_i^2}A_{ij}-\frac{\boldsymbol{\sigma}^{\alpha,\beta}(\boldsymbol{x}_i)}{\rho_j^2}A_{ji}\right\}. \tag{2}$$

Conservation equation of energy:

$$\frac{\mathrm{d}E}{\mathrm{d}t}(\boldsymbol{x}_i)=-\frac{P_i}{\rho_i^2}\sum_{j=1}^{N}m_j(\boldsymbol{v}(\boldsymbol{x}_j)-\boldsymbol{v}(\boldsymbol{x}_i))A_{ij}. \tag{3}$$

In Eqs.(1)~(3), $\rho$ is the density, $m$ is the mass, $\boldsymbol{v}$ is the spatial velocity, $E$ is the energy, $\boldsymbol{\sigma}$ is the stress tensor, $\boldsymbol{x}_i$ is the position vector for particle $i$, $\alpha$ and $\beta$ are the space indices, $A_{ij}$ is the operator including kernel function and can be written as

$$A_{ij}=\frac{\boldsymbol{x}_i-\boldsymbol{x}_j}{r_{ij}}\frac{\partial W_{ij}}{\partial r_{ij}},$$

where $r_{ij}$ is the distance from particle $i$ to particle $j$, $W$ is the kernel function.

### Coupling algorithm of SPH with FEM

To make the most of advantages of both SPH and FEM, the coupling between SPH and FEM is needed. In general, the coupling algorithm is based on a master-slave algorithm to account for the contact interaction of FE and SPH particles (de Vuyst *et al*., 2005). The contact algorithm will detect when a particle penetrates the segments of the surface of the FE. The contact thickness indicates the distance away from a contact face where physical contact is established. Whenever a node enters this detection region, it is repelled by a force that is a function of the predicted penetration.

In the present study, because the near field (SPH region) and far field (FE region) are the same soil medium, SPH particles are joined with FEs as a single node in the calculation. They will remain exactly together throughout the calculation unless the join condition is removed (Fig.1). An interface constraint between FE and SPH regions is reduced to standard FE shape functions and poses the Kronecker delta property as follows:

$$\tilde{\Psi}_i=0\ (\boldsymbol{x}\in\Gamma_{\text{interface}}),$$

where $\tilde{\Psi}_i$ is the modified coupled FE and SPH function for the node $i$, $\Gamma_{\text{interface}}$ is the interface between the FE and SPH regions.

It is important that the order of the FE interpolation is chosen to be the same as that of the kernel function. In addition, near field, the extreme deformation region, can be estimated through empirical functions or the trial computation in advance.

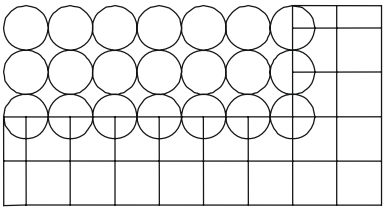

**Fig.1 Coupling of SPH to FEM**

### Solution of two SPH materials

The soil surrounding the explosive charge where severe deformation occurs and the charge are modeled using SPH region. It is unnecessary to define a contact between SPH parts when two SPH materials

exist in the same model. The contact between two SPH materials will occur when particles of the first part will be located in the sphere of influence of particles of other parts.

## CONSTITUTIVE MODEL

### Soil model

According to the behavior of soil, the Drucker-Prage model (Drucker *et al*., 1952) is employed for analysis of structures. Its yield function is described as

$$F = \alpha \boldsymbol{I}_1 + \sqrt{\boldsymbol{J}_2} = k, \tag{4}$$

where $\boldsymbol{I}_1$ is the first invariant of the stress tensor; $\boldsymbol{J}_2$ is the second invariant of the deviatoric stress tensor; $\alpha$ is the angle of friction; $k$ is the cohesion. Model parameters of $\alpha$ and $k$ are computed by using the Mohr-Coulomb strength parameters of the friction angle $\varphi$ and cohesion $c$, respectively. They can be expressed as

$$\boldsymbol{I}_1=\boldsymbol{\sigma}_1+\boldsymbol{\sigma}_2+\boldsymbol{\sigma}_3, \tag{5}$$

$$\boldsymbol{J}_2=[(\boldsymbol{\sigma}_1-\boldsymbol{\sigma}_2)^2+(\boldsymbol{\sigma}_1-\boldsymbol{\sigma}_3)^2+(\boldsymbol{\sigma}_2-\boldsymbol{\sigma}_3)^2]/6, \tag{6}$$

$$\alpha = \frac{2\sqrt{3}\sin\varphi}{\sqrt{2\sqrt{3}\pi(9-\sin^2\varphi)}}, \tag{7}$$

$$k = \frac{6\sqrt{3}c\cos\varphi}{\sqrt{2\sqrt{3}\pi(9-\sin^2\varphi)}}. \tag{8}$$

### Material model for concrete

The damage of concrete can be caused by blast loads. In addition, the strain rate has an influence on the behavior of concrete. The RHT model developed by Riedel, Hiermaier and Thoma in Ernst Mach Institute (Riedel *et al*., 1999) is adopted for the present dynamic analysis. The model can be split into four components, namely the failure surface, the elastic limit surface, the residual failure surface and damage model. The part for strength model can be found in (Riedel *et al*., 1999; Wang *et al*., 2005).

In damage model, additional plastic straining of the material leads to damage and strength reduction following the hardening phase. Damage is accumulated by

$$D = \sum \frac{\Delta\varepsilon_{\mathrm{pl}}}{\varepsilon_{\mathrm{p}}^{\mathrm{failure}}}, \tag{9}$$

$$\varepsilon_{\mathrm{p}}^{\mathrm{failure}} = D_1(p^* - p_{\mathrm{spall}}^*)^{D_2} \geq \varepsilon_{\mathrm{f}}^{\min}, \tag{10}$$

where $\varepsilon_{\mathrm{pl}}$ is the current plastic strain, $D_1$, $D_2$ are damage constants, $p^*$ is the pressure normalized by the compressive strength, $p_{\mathrm{spall}}^*$ is the strain rate function, and $\varepsilon_{\mathrm{f}}^{\min}$ is the minimum strain to reach failure.

The post-damage failure surface is then interpolated by

$$Y_{\mathrm{fracture}}^* = (1-D)Y_{\mathrm{failure}}^* + DY_{\mathrm{residual}}^*, \tag{11}$$

and the post-damage shear modulus is interpolated by

$$G_{\mathrm{fracture}} = (1-D)G_{\mathrm{initial}} + DG_{\mathrm{residual}}, \tag{12}$$

where $Y_{\mathrm{failure}}^*$ and $Y_{\mathrm{residual}}^*$ are the current failure surface and residual failure surface, respectively. $G_{\mathrm{initial}}$ and $G_{\mathrm{residual}}$ are initial and residual shear moduli, respectively.

For the volumetric compaction, the Herrmann (1969)'s $P$-$\alpha$ model is used as the equation of state for concrete material.

### High explosives

In order to accurately attain the location and the magnitude of explosive load, and to avoid the shortcoming of simplification where the explosive load is generally considered as a loading function, blast analysis is needed. We applied the Jones-Wilkins-Lee (JWL) equation of state to high explosive proposed by Lee *et al*.(1968) assuming ideal stationary detonation. The equation of state is

$$P = A\left(1-\frac{\omega}{R_1V}\right)\mathrm{e}^{-R_1V} + B\left(1-\frac{\omega}{R_2V}\right)\mathrm{e}^{-R_2V} + \frac{\omega E}{V}, \tag{13}$$

where $V$ is the specific volume; $E$ is specific energy; $A$, $B$, $R_1$, $R_2$ and $\omega$ are constants of various common explosives.

## NUMERICAL INVESTIGATION

To validate the parameters used in material models and the coupled SPH-FEM approach, the blast analysis for free field is firstly performed and the result is compared with empirical equations. On basis of the validation, the structural performance under subsurface blast is reproduced, and some helpful conclusions are addressed.

### Free field blast analysis

Pillarlike explosive charge, 33.2 kg, is embedded at 3.0 m deep in the infinite soil medium. It is simplified to an axis symmetrical problem. The explosive charge and the extreme deformation soil medium are modeled by SPH region, while FEM elements are used to model the far soil and the structure (Wang *et al*., 2005). Transmission boundaries are applied. Mechanical properties used for both soil and charge are shown in Table 1 and Table 2, respectively. In Table 1, PCJ is the initial C-J pressure; VOD is the C-J detonation velocity.

**Table 1 Parameters for explosion generation**

| Parameter | Value | Parameter | Value |
|---|---|---|---|
| $A$ (GPa) | 3.72 | $\omega$ | 0.3 |
| $B$ (GPa) | 3.53 | $\rho_0$ (kg/m$^3$) | 1.63×10$^3$ |
| $R_1$ | 4.15 | *VOD* (m/s) | 6950 |
| $R_2$ | 0.95 | *PCJ* (GPa) | 28 |

**Table 2 Mechanical properties of soil**

| Parameter | Value | Parameter | Value |
|---|---|---|---|
| $\rho$ (kN/m$^3$) | 18.0 | $G$ (MPa) | 0.0036 |
| $E$ (GPa) | 0.01 | $\alpha$ (°) | 15.8 |
| $C$ (GPa) | 0.04 | | |

Fig.2 shows variations of the peak pressure and the peak velocity at different points of the soil medium. It can be seen that the peak pressure and the peak velocity fall rapidly with the increase of distance from charge. The peak pressure and the peak velocity by the presented SPH-FEM approach are consistent with those by corresponding empirical equations (Lu *et al*., 2005).

The evolution of the shape of the crater at different time ($t$=2.5, 9.6 and 39.0 ms) is shown in Fig.3. It can be seen that the crater equably expands outward at the beginning of explosion, and that the initial shape of crater gradually turns to be circular and then is changed by reflection wave after the impulse wave reaches the free surface. It agrees well with the general recognition of explosives.

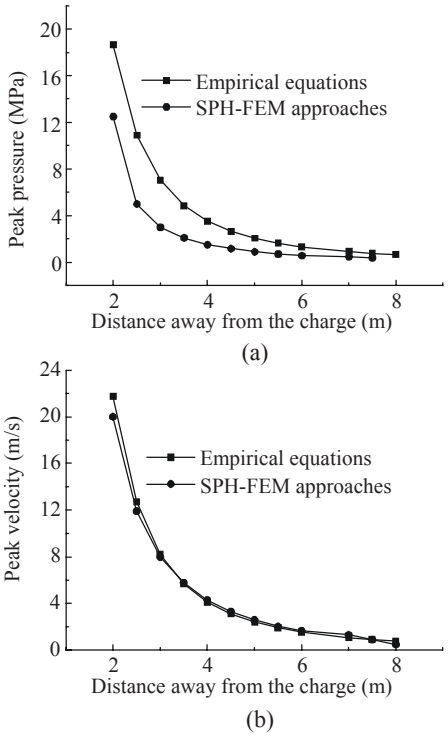


**Fig.2 Variations of the (a) peak pressure and (b) peak velocity at different locations**

### Response of structures subjected to subsurface blast

The response of a three-storey, three-bay reinforced concrete frame, with the height of 11.8 m and the width of 14.0 m, is simulated under subsurface blast. The numerical model and location of target points are shown in Fig.4. As it can be seen in this figure, the explosive charge of 400 kg of TNT is embedded at 1.25 m deep. The horizontal distance from the front of the building to the charge is 2.5 m. The frame columns dimensions are the same from ground to upper story, and all beams have the same dimensions and reinforcement layout. Mechanical properties of the soil and the charge are the same as the former example. Since it is impracticable in a simulation for the complete structure to take into account all the reinforcement details, the tensile strength of concrete is increased to resist tension stresses (Luccioni *et al*., 2004). Properties of reinforced concrete are listed in Table 3.

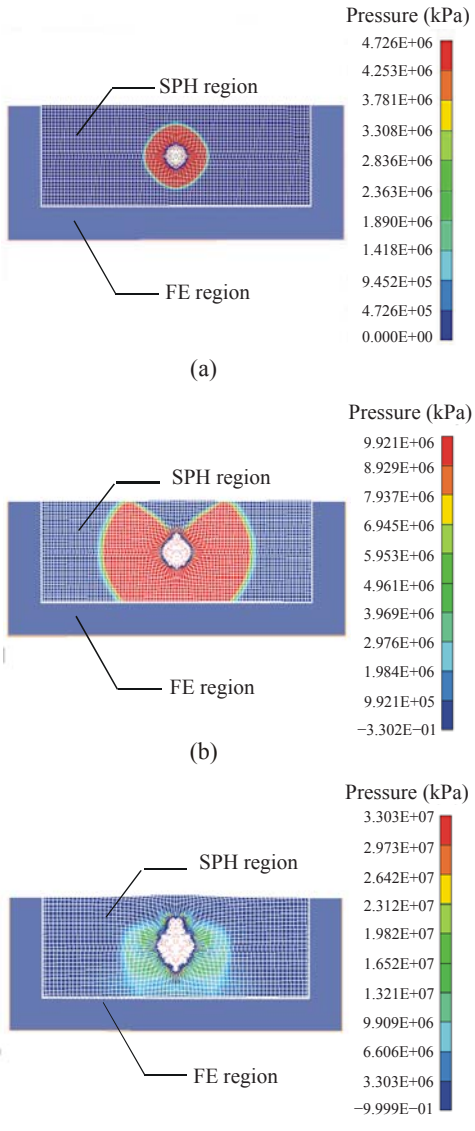


**Fig.3 Formation of crater in free field. (a) $t$=2.5 ms; (b) $t$=9.6 ms; (c) $t$=39.0 ms**

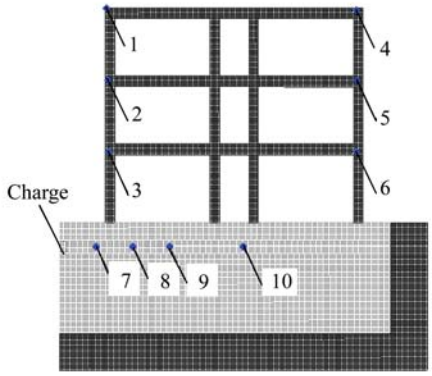


**Fig.4 Numerical model using coupled SPH-FEM approach and location of target points**

**Table 3 Mechanical properties for reinforced concrete model**

| Parameter | Value | Parameter | Value |
|---|---|---|---|
| $f_c$ (MPa) | 35 | $D_1$ | 0.04 |
| $f_t$ (MPa) | 10 | $D_2$ | 1.0 |
| $A$ | 1.6 | $\varepsilon_f^{\min}$ | 0.01 |
| $N$ | 0.61 | $P_e$ (MPa) | $2.33\times10$ |
| $n_1$ | 0.036 | $P_s$ (MPa) | $6.0\times10^3$ |
| $n_2$ | 0.032 | $G_{initial}$ (Mpa) | $1.67\times10^4$ |
| $Q_{2,0}$ | 0.61 | $G_{residual}$ (Mpa) | $2.17\times10^3$ |
| $B$ | 1.6 | $\varepsilon_{pl}$ | $1.93\times10^{-3}$ |
| $M$ | 0.61 | | |

1. Propagation of pressure wave in structural foundation

Right after the detonation, a pressure wave is generated in the soil medium. The overpressure histories of selected targets are shown in Fig.5. It can be seen that, the overpressure decreases gradually with

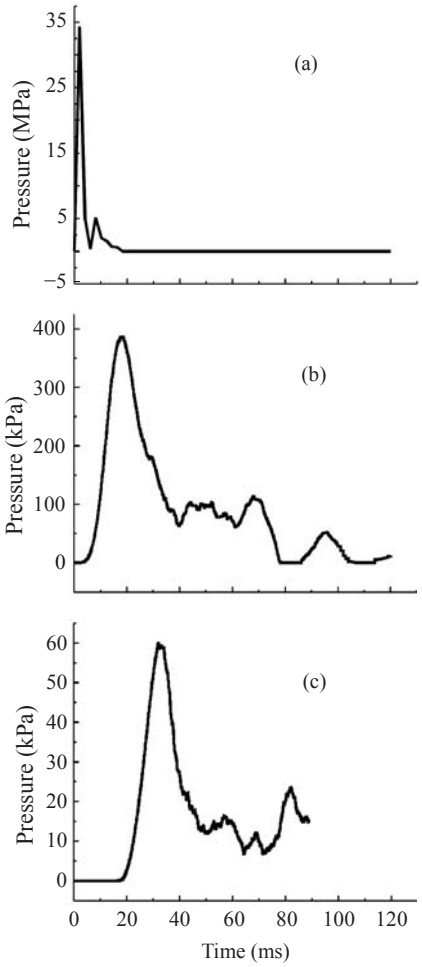


**Fig.5 Pressure-time history at different targets in soil medium. (a) Target 7; (b) Target 9; (c) Target 10**

the increasing distance. Hence, one of the most effective means to protect structures is to increase the distance between a potential bomb and the building to be protected.

The acceleration histories at Target 8 in Fig.4 are shown in Fig.6. It is obvious that the horizontal acceleration is larger than the vertical one. For the vertical acceleration, the negative acceleration is smaller than the positive one. This indicates that the acceleration in the soil is sensitive to a free surface. It should be noted also that the duration of shock wave induced by blast loads is about 50 ms in the present case. However, it is generally known that the duration of earthquake is about 10 s. In the sense, the hazard from the earthquake is severer than that from explosion.

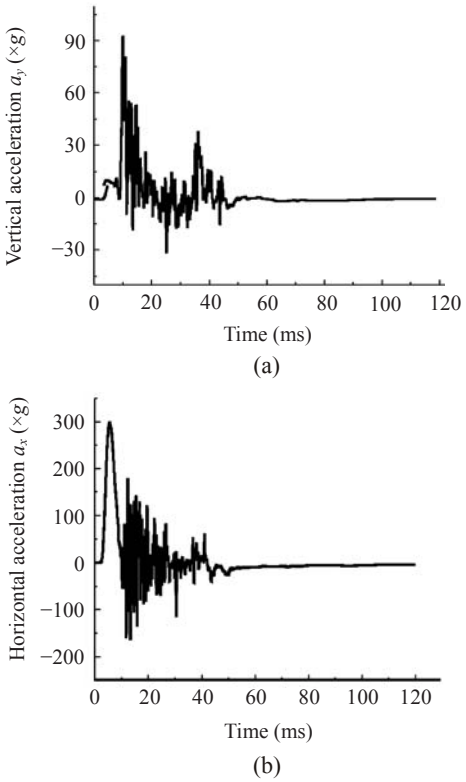


**Fig.6 Acceleration-time history at Target 8 in soil. (a) Vertical acceleration; (b) Horizontal acceleration**

The unphysical oscillations of the pressure profiles were found from Figs.5~6. Generally, it is caused by time step, the predefined number of neighbor particles, the artificial viscosity coefficient, material interfaces, and so on. The further description can be seen in (Liu *et al*., 2003). The errors from the numerical oscillations can be reduced by adjustment of the above parameters. According to the validation of free field blast analysis in subsection "Free field blast analysis", the numerical oscillations are acceptable compared to the magnitude of the shock wave.

2. Structural responses

The velocity and acceleration are also two important indices for assessment of shock environment in building under blast loads. Fig.7 shows the acceleration histories of selected target points on the structure. It can be seen that the acceleration behind the structure is generally on a lower order than those in the front face. For example, the maximum acceleration at Target 1 is about 40*g*, while it is only 4*g* at Target 4. Fig.8 plots the horizontal displacement histories at Target 1 showing the maximum value is 0.56 mm. The short duration is the main reason for such small displacement notwithstanding the maximum acceleration on the structure reaches the order of 40*g*~60*g*. The similar characteristic of the structural performance under explosive loads is also showed by Lu and Wang (2006).

Because the distance from the charge center to the free surface is shorter and the mass of charge is larger than those of free field cases in subsection "Free field blast analysis", the energy released by explosive overcomes the bafflement of the soil over the charge and the ejecting of the soil occurs. The explosive process is shown in Fig.9. It can be seen that ground level over the charge rises up firstly, then the uplifted height increases and the area of the crater is extended with time. It is obvious that the foundation near the foot of front column suffers severe damage, whereas the structural damage cannot be found. The progressive collapse of the structure reduced by the destruction of the foundation is not discussed in the present study.

In order to compare the damage to the structure subjected to above-ground explosions with foregoing case, another simulation using the coupled Lagrangian-Eulerian method is performed. The charge is located 1.25 m above the ground level, while other conditions keep unchanged. It represents a kind of vehicle carried explosives. Properties of air are list in Table 4, and the equations of state for the air are

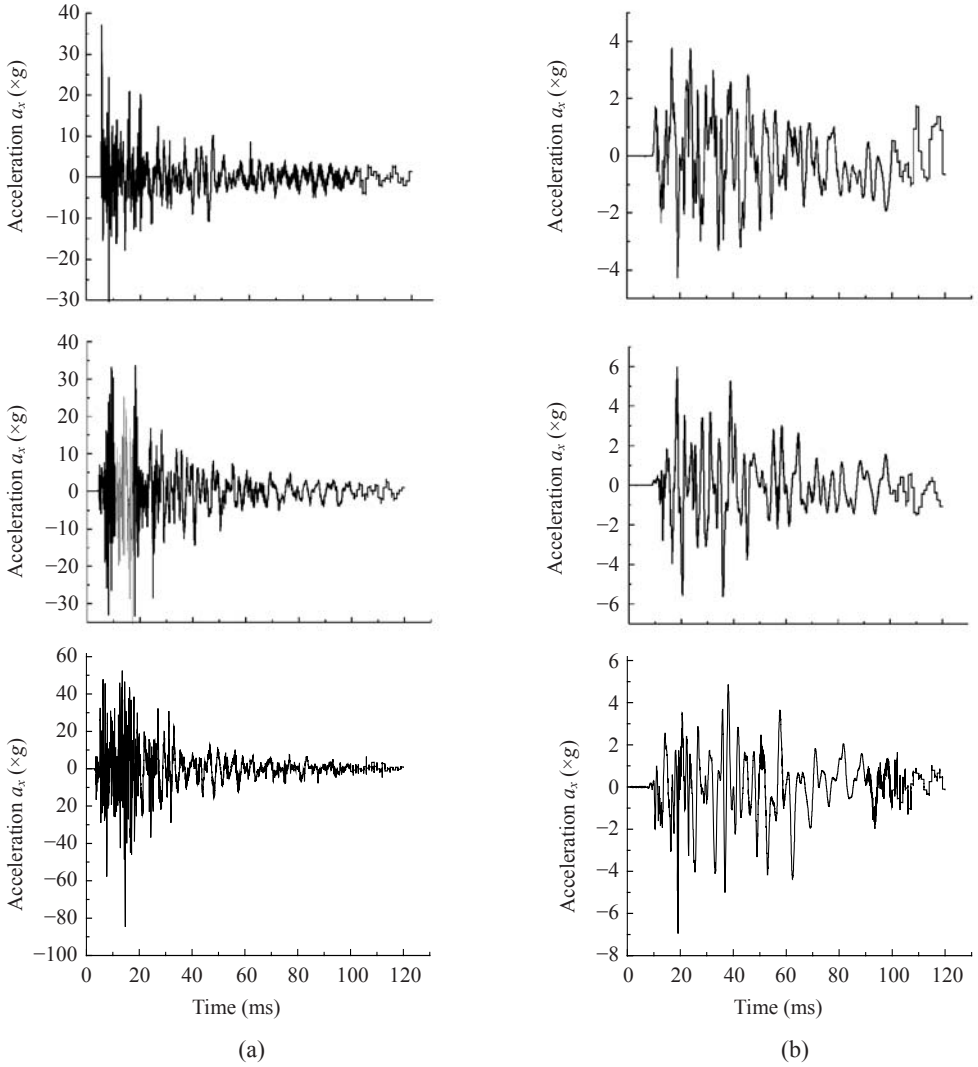


**Fig.7 Time history of horizontal acceleration at different targets on structures. (a) Targets 1~3; (b) Targets 4~6**

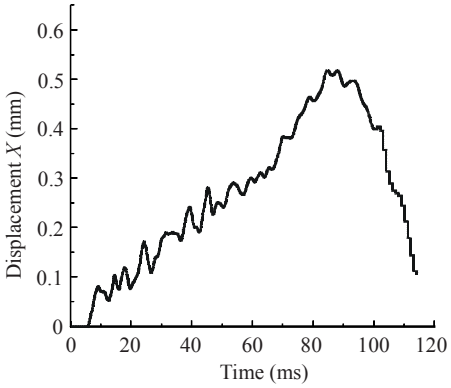


**Fig.8 Time history of horizontal displacement at Target 1 on the structure**

$$p = (\gamma - 1)\rho e, \tag{14}$$

$$e = C_v T, \tag{15}$$

where $p$ is the pressure, $\rho$ is the density, $\gamma$ is a constant, $e$ is the internal energy, $C_v$ is the specific heat, $T$ is the temperature.

The computation reveals that the structures were destroyed after the pressure wave reached them. The damage contour of the front face of structures is shown in Fig.10. The front columns of the first-storey are almost completely destroyed leaving the upper


**Fig.9 Simulations of subsurface blast processes. (a) $t$=3.8 ms; (b) $t$=15.0 ms; (c) $t$=82.6 ms**

**Table 4 Properties of air**

| Parameter | Value |
|---|---|
| Constant $\gamma$ | 1.41 |
| Reference density (g/cm$^3$) | $1.225\times10^{-3}$ |
| Reference temperature (K) | 288.20 |
| Specific heat (J/(kg·K)) | 717.3 |

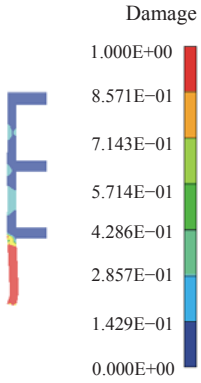


**Fig.10 Damage contour of the front face of structures**

beams without support. The damage to structures under consideration is much severer than that subjected to the subsurface blast despite their masses of TNT are the same, but just the reverse is true for the damage to the foundation.

## CONCLUSION

A numerical model using the coupled SPH-FEM approach is presented for analysis of structural response to blast loads. This model covers some key issues including the coupling of SPH with FEM, the selection of appropriate material models and the simulations of explosive loads. Two examples are employed and demonstrate the advantage of the coupled SPH-FEM approach on the simulation of larger deformations.

For free field explosive analysis, the comparisons of numerical results with empirical equations show that the numerical model can reasonably and efficiently predict the structural response to blast loads.

The study reveals that the acceleration in the soil is sensitive to a free surface. In addition, the shape of crater varies with the depth of embedded charges. The distribution of in-structure shock environment is obtained through the study of acceleration-time histories. It is helpful for the personnel protection in building under blast loads. For explosive loads with the same mass of TNT, the damage to structures under aboveground explosion is much severer than that under subsurface blast, and this indicates that soil layer works more effectively in absorbing stress wave energy.

## References

Century Dynamic Inc., 1998. Autodyn Theory Manual, San Ramon, California.

de Vuyst, T., Vignjevic, R., Campbell, J.C., 2005. Coupling between meshless and finite element method. *International Journal of Impact Engineering*, **31**(8):1054- 1064. [doi:10.1016/j.ijimpeng.2004.04.017]

Drucker, D.C., Prager, W., 1952. Soil mechanics and plastic analysis or limit design. *Quarterly of Applied Mathematics*, **10**(2):157-164.

Du, Y.X., Liu, J.B., Wu, J., Du, X.L., 2006. Blast shock and vibration of underground structures with conventional weapon. *Journal of Tsinghua University (Science and Technology)*, **46**(3):322-326 (in Chinese).

Gingold, R.A., Monaghan, J.J., 1977. Smoothed particle hydrodynamics: theory and application to non-spherical stars. *Royal Astronomical Society*, **181**:375-389.

Herrmann, W., 1969. Constitutive equation for the dynamic compaction of ductile porous material. *Journal of Applied Physics*, **40**(6):2490-2499. [doi:10.1063/1.1658021]

Lee, E.L, Hornig, H.C., Kury, J.W., 1968. Adiabatic Expansion of High Explosive Detonation Products. Lawrence Radiation Laboratory, University of California.

Liu, M.B., Liu, G.R., Lam, K.Y., Zong, Z., 2003. Smoothed particle hydrodynamics for numerical simulation of underwater explosion. *Computational Mechanics*, **30**(2): 106-118. [doi:10.1007/s00466-002-0371-6]

Lu, X.Z., Jiang, J.J., 2001. Dynamic finite element simulation for the collapse of world trade center. *China Civil Engineering Journal*, **34**(6):8-10 (in Chinese).

Lu, Y., Wang, Z.Q., 2006. Characterization of structural effects from above-ground explosion using coupled numerical simulation. *Computers and Structures*, **84**(28):1729-1742. [doi:10.1016/j.compstruc.2006.05.002]

Lu, Y., Wang, Z.Q., Chong, K., 2005. A comparative study of buried structure in soil subjected to blast load using 2D and 3D numerical simulations. *Soil Dynamics and Earthquake Engineering*, **25**(4):275-288. [doi:10.1016/j.soildyn.2005.02.007]

Luccioni, B.M., Ambrosini, R.D., Danesi, R.F., 2004. Analysis of building collapse under blast loads. *Engineering Structures*, **26**(1):63-71. [doi:10.1016/j. engstruct.2003.08.011]

Lucy, L.B., 1977. A numerical approach to the testing of the fission hypothesis. *The Astronomical Journal*, **82**:1013-1024. [doi:10.1086/112164]

Riedel, W., Thoma, K., Hiermaier, S., 1999. Numerical Analysis Using a New Macroscopic Concrete Model for Hydrocodes. Proceedings of 9th International Symposium on Interaction of the Effects of Munitions with Structures, Berlin, p.315-322.

Wang, Z.Q., Lu, Y., Hao, H., Chong, K., 2005. A full coupled numerical analysis approach for buried structures subjected to subsurface blast. *Computers and Structures*, **83**(4-5):339-356. [doi:10.1016/j.compstruc.2004.08.014]